Sol-gel preparation of a silica antireflective coating with enhanced hydrophobicity and optical stability in vacuum

Qinghua Zhang (张清华)*, **Lian Zhou (周 炼)**, **Wei Yang (杨 伟)**, **Haohao Hui (惠浩浩)**,
Jian Wang (王 健), and **Qiao Xu (许 乔)**

Chengdu Fine Optical Engineering Research Centre, Chengdu 610041, China
*Corresponding author: zhangqh506@gmail.com
Received January 21, 2014; accepted April 23, 2014; posted online June 25, 2014

A new silica antireflective coating with improved hydrophobicity and optical stability in a vacuum is obtained by a two-step route. Firstly, silica sols are prepared with a sol-gel process, in which tetraethyl orthosilicate is utilized as a precursor. And by introduction of fluorine containing glycol into the sols, the porosity of silica particles and surface polarity of the coatings are decreased. Afterward, coatings are constructed with low surface roughness by modification of PMBA-PMMA. The coatings retain transmission of up to 99.6%, and laser damage threshold of about 50 J/cm^2 at a wavelength of 532 nm (1-on-1, 10 ns).

Sol-gel process derived silica antireflective (AR) coatings are well applied on optical transmissive elements in high power laser systems[1−4]. However, the sol-gel silica AR coating is composed of porous silica particles with much hydroxyl groups on its surface, which easily absorbs water and volatile organic compounds from environment. This absorption is detrimental to the optical performance, which not only reduces the AR efficiency, but also decreases the laser damage threshold of the AR coatings. There are many attempts to hinder the adsorption of contamination either by deactivation of polar hydroxyl groups on the surface of silica particles or by introducing hydrophobic groups into sol systems[5,6].

In this letter, silica sols were prepared using 1H, 1H, 11H, 11H-perfluoro-3, 6, 9-trioxandecane-1, 11-diol (FTG) to control the porosity and stacking manner of the silica particles. And with the existence of this fluorine-containing compound in the pore of silica particles, the hydrophobicity of the coatings was increased to a certain degree. Then the FTG/silica sol was modified by the copolymer of poly (butyl methacrylate) and poly (methyl methacrylate) (PMBA-PMMA), thus the hydrophobicity of the silica coating was improved further. The optical property and 532-nm laser damage threshold of the modified silica coatings were investigated.

Colloidal silica sol was prepared by the hydrolysis and condensation of tetraethyl orthosilicate (TEOS) in deionized water and anhydrous ethanol, which was catalyzed by ammonium hydroxide. Different amounts of FTG were added in, and the weight ratios of FTG to TEOS were 0%, 1%, 2%, 3%, 4%, and 6%, respectively. After being stirred at room temperature for 6 h, the resultant sol was aged at 25 °C for 14 days. Then, assisted by ultrasonic, the PMBA-PMMA was dissolved in a mixture of acetone and sec-butyl alcohol, which was added in the silica sols for modification. The weight ratios of PMBA-PMMA to TEOS were 0.5%, 1%, 2%, and 4%, respectively. These sols were deposited on well cleaned fused silica substrates by dip-coating. In order to obtain the refractive indices of the coatings before and after modification, the silica sols were deposited on silicon substrates by dip-coating at the same withdrawal rate. All of the coatings were then heated at 180 °C for 24 h.

As shown in Fig. 1, the Fourier transmission infrared (FTIR) spectra of PBMA-PMMA reveal that the absorption peak at 1724 cm^{-1} are attributed to C=O asymmetric stretching mode, while the absorption peak at 748 cm^{-1} are assigned to bending vibration of –(CH$_2$)$_3$– group. In the spectra of FTG/PMBA-PMMA/silica, further absorption peaks located at 1724 and 748 cm^{-1} indicate the existence of PMBA-PMMA compound in this silica particles. The absorption band recorded at 1284 cm^{-1} corresponds to bending mode of C–F in FTG compound[7], while the peak 862 cm^{-1} are attributed to asymmetric bending mode of C–O–C. As shown in the spectra of FTG/PMBA-PMMA/silica, the appearance of these characteristic absorption peaks indicates the existence of FTG compound in the silica particles In the spectra of FTG/PMBA-PMMA/silica and pure silica, the strong absorption band at about 1100 cm^{-1} is ascribed to the stretching modes of the Si–O–Si bonds. The bands at 796 cm^{-1} are assigned to the symmetric Si–O stretching mode[8].

During the formation of the sol particles, ethoxyl groups in TEOS hydrolyzed, the hydrogen atom in these hydroxyl groups may take priority to form hydrogen bonds with fluorine atoms in FTG molecules. By forming hydrogen bond with FTG molecules, those partially hydrolyzed TEOS molecules may be arranged together. Their remaining ethoxly groups may hydrolyze and condense. Hence, the particle structure in the FTG/silica sol is denser than that in the pure silica sol. With some FTG molecules distributed across the surface of final silica particles, the boundary of these particles is regular and clear as shown in Figs. 2 (a) and (b).

For an AR coating prepared from silica sol, the sol particle size and structure are key factors which affect the refractive index of the AR coatings. By controlling refractive index and thickness, the reflection of AR coatings can nearly reach 0% at specific wavelengths. As shown in Table 1, in the series of FTG/silica AR coatings, an increase of refractive index from 1.219 to 1.245 is
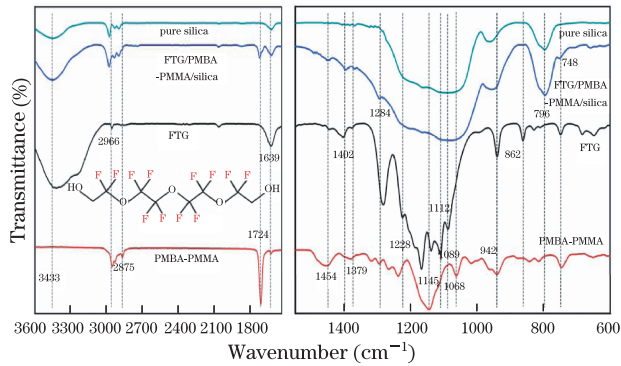
Fig. 1. FTIR spectra of pure silica, modified silica, FTG, and PMBA-PMMA.
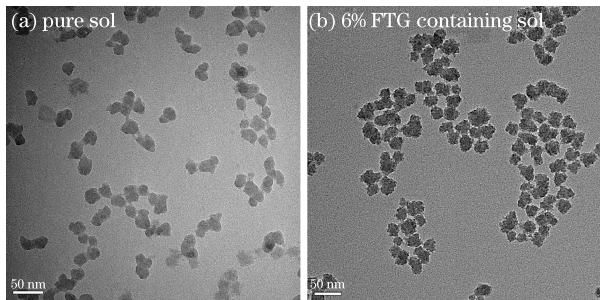

Fig. 2. TEM pictures of (a) pure silica sol and (b) 6% FTG containing sol.

found when the FTG concentration increases from 0% to 6%. This is attributed to the size, porosity, and stacking manner of silica particles in the coating. As shown in Fig. 3(c), in the FTG-containing coatings, it seems that the size and density of silica particles are much higher, and the particle shape and stacking pattern are more regular than that in the pure silica coatings. The silica particles in the FTG-containing coatings are arranged more compact and regular than that of pure silica coatings. With such a regular arrangement of silica particles in FTG/silica sol, the refractive indices are larger than

that of pure ones.

As shown in Figs. 3(b) and (d), when modified by PMBA-PMMA, the polymer filled into the inter-particle spacing of the sols. As shown in Table 1, with the increase of PMBA-PMMA concentration from 0.5% to 4%, the refractive indices of pure silica AR coatings and 6% FTG-containing silica AR coatings increased from 1.222 to 1.236 and 1.247 to 1.260, respectively. After PMBA-PMMA modification, the pores between silica particles are filled with the compound which lowers the porosity of the coatings, and hence increases the refractive indices.

Three-dimensional AFM images of pure silica AR coatings and 6% FTG-containing silica AR coatings modified by 4% of PMBA-PMMA are shown in Fig. 4. All coating surfaces are composed of conjoint island and show rugged characteristic. For the pure silica coatings, its surface is composed of lots of small islands and shows highest porous structure. Compared with pure silica sol, silica particles in the FTG/silica sol were linked together and formed larger clusters as shown in Fig. 4. From AFM images, it can be found that the surface of the FTG-containing coating is somewhat rougher and the density of pores decreases. As shown in Fig. 4, more compact structures have been formed in PMBA-PMMA modified silica coatings than that in pure ones. As shown in Fig. 4(d), the FTG/PMBA-PMMA/silica coating seems to be composed of large aggregates with size of about 200 nm, whose surface is most rugged in these four samples. This coating morphology may be due to existence of rigid particle clusters enwrapped by PMBA-PMMA compound in FTG/PMBA-PMMA/silica coating.

As an important property of optics, the surface roughness of the coatings was tested. As shown in Fig. 5, the surface roughness is actually related to small particles. The surface roughnesses of pure silica coating, PMBA-PMMA/silica coating, FTG/silica coating, and FTG/PMBA-PMMA/silica coating are 0.93, 0.74, 1.05 and 1.20 nm, respectively. With such a smooth surface, the scatter losses of these silica coatings are nearly neglectable.

Table 1. Refractive Indices at 532 nm, Coating Thickness, and Transmittance of the AR Coatings before and after Modification

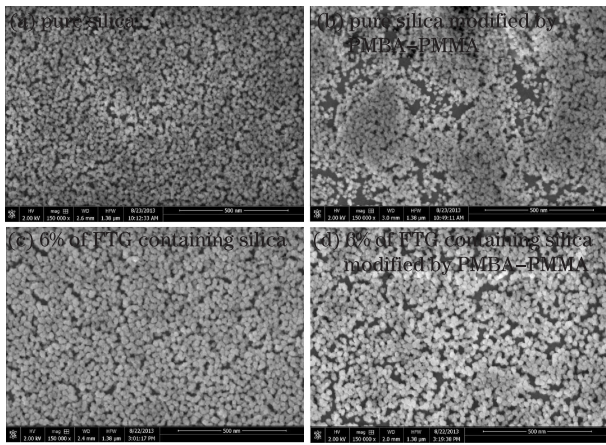| W% (FTG/TEOS)	FTG/Silica Coatings			W% (PMBA-PMMA/TEOS)	FTG/PMBA-PMMA/Silica Coatings		
	Refractive Index n	Coating Thickness (nm)	T_{532} (%)		Refractive Index n	Coating Thickness (nm)	T_{532} (%)
0	1.219	111	99.9	0.5	1.222	115	99.9
				1	1.225	112	99.9
				2	1.228	109	99.9
				4	1.236	108	99.8
1	1.227	108	99.9				
2	1.228	107	99.9				
3	1.237	107	99.8				
4	1.238	105	99.8				
6	1.245	105	99.6	0.5	1.247	108	99.6
				1	1.249	106	99.6
				2	1.251	104	99.5
				4	1.260	100	99.5

Fig. 3. FIB-SEM pictures of pure silica coating with a magnification of (a) 100000 and (b) 150000; PFG-containing silica coating with a magnification of (c) 100000 and (d) 150000.
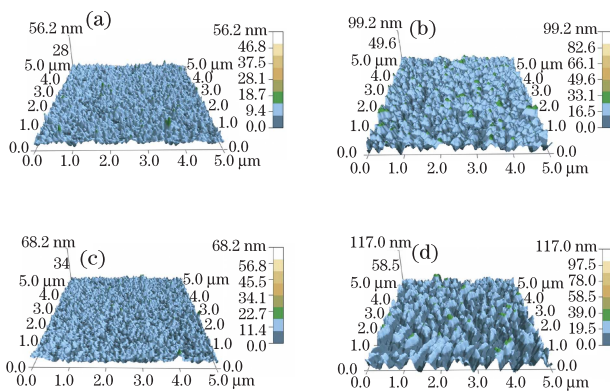

Fig. 4. Surface morphologies of (a) pure silica AR coatings, (b) pure silica AR coatings modified by 4% of PMBA-PMMA, (c) 6% of FTG containing silica AR coatings, and (d) 6% of FTG containing silica AR coatings modified by 4% of PMBA-PMMA.
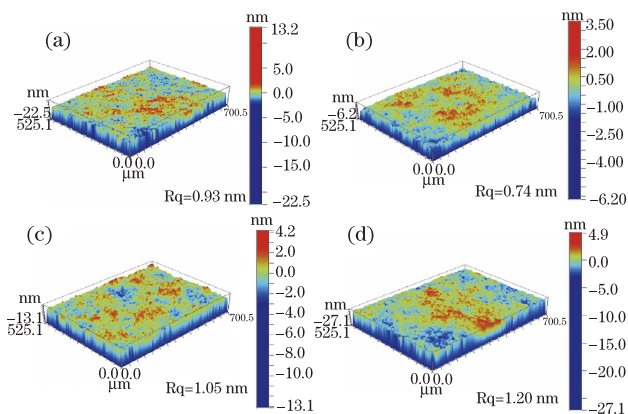

Fig. 5. Surface roughness of silica coatings. (a) pure silica; (b) PMBA-PMMA modified pure silica; (c) 6% FTG-containing silica; (d) PMBA-PMMA modified 6% FTG-containing silica.

Hydrophobic nature of a silica thin film is closely linked to the AR durability of the AR coating. The hydrophobicity can be represented by the water contact angle. The contact angles of water droplets on the surface of silica coatings were monitored. Figure 6(a) shows the water contact angles of the silica AR coating with different contents of FTG. With the increase of weight ratio

of FTG to TEOS, the water contact angle increases from 36° to 96°, which indicates an obvious increase in the hydrophobicity of AR coating after introducing FTG. During the formation of silica particles, with some FTG molecules distributed across the surface of final silica particles, the surface energy of the surface were decreased. As a hydrogen bond acceptor, fluorine atoms may form hydrogen bond with hydrogen atoms in the hydroxyl groups on the surface of silica particles, which lowers the polarity of the coating surfaces.

With the introduction of PMBA-PMMA compound into the silica sol, the PMBA-PMMA molecules fill in the inter-particle voids, which decreasees the porosity of the silica AR coatings. As shown in Fig. 6(b), while the concentration of PMBA-PMMA in 6% FTG-containing sol increases from 0% to 4%, the water contact angles of the coatings increase from 96° to 119°. There are some explanations that the hydrophobicity of the coatings is dominated by surface morphology[9]. As for the FTG-containing coating before and after PMBA-PMMA modification, in addition to the influence of surface energy, the surface roughness might be a main factor for coatings' hydrophobicity. Owing to such more densely packed aggregates of particles and larger pits, the FTG/PMBA-PMMA/silica coating surface will contact water droplets with smaller adhesion focal and force, which produces more hydrophobic surface than FTG/silica as well as PMBA-PMMA/silica.

The fused silica substrates coated with modified and pure silica were kept in a vacuum chamber of 0.15 MPa which was connected with an oil pump via a valve. With two fused silica substrates coated with modified silica and two with pure silica as a group, four groups of coating were prepared at the same time. The transmittance of the first group was measured as soon as they were finished, and the remaining three groups were placed in the vacuum chamber and their transmittances were measured after 3, 7, and 10 days, respectively. The evolution of the peak transmission due to contamination is shown in Fig. 7. The transmittance of 6% FTG and 4% PMBA-PMMA containing silica coatings changed from 99.5% to 99.1%, while that of pure silica coatings decreased dramatically from 99.9% to 97.1% during 10 days of contamination exposure. The organic contaminants in this vacuum chamber were characterized by GC-MS method, which were gathered by rinsing the fused silica samples once placed in vacuum chamber with chromatographic pure toluene. And the GC-MS characterization result showed that the organic contaminants were mainly cyclohexane, cyclopentane, alkanes, and alkenes with 9 to 12 carbon atoms, which might volatilized from vacuum
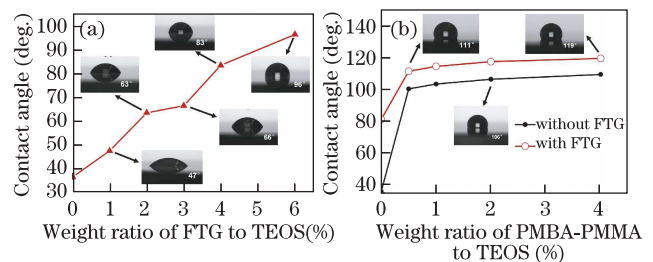

Fig. 6. Water contact angle versus (a) FTG and (b) PMBA-PMMA concentrations.
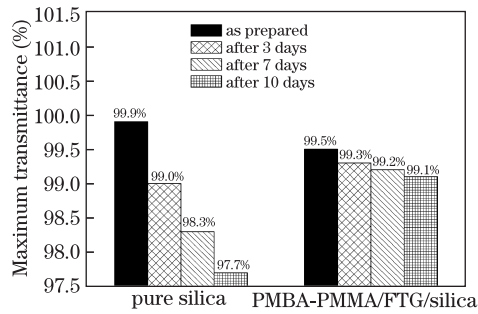
Fig. 7. Changes in maximum transmittance as function of test time in a vacuum chamber of 0.15 MPa.
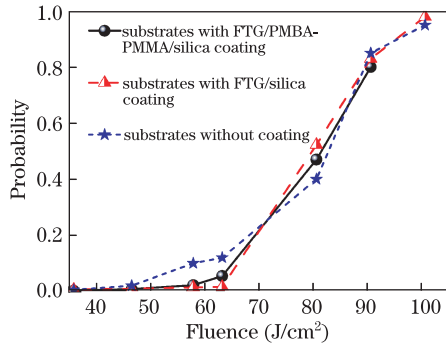

Fig. 8. Damage probability of the silica substrates with and without silica AR coatings. 532 nm, 10 ns, at the incidence of $0°$.
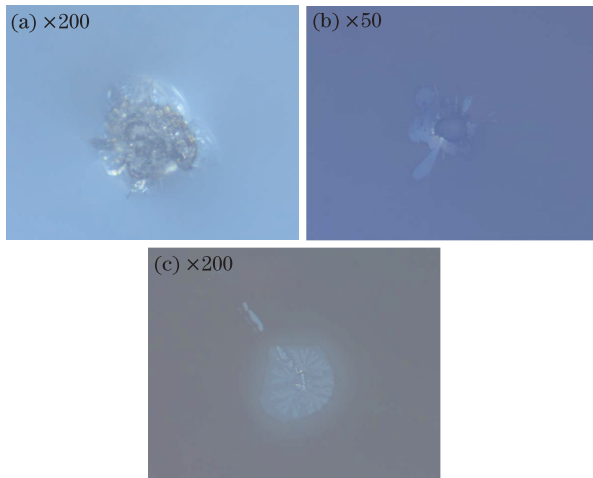

Fig. 9. Damage morphology of silica substrates (a) without coating, (b) with pure silica AR coating, and (c) with FTG/PMBA-PMMA/silica AR coating.

pump oil. The incorporation of FTG and PMBA-PMMA significantly improves the optical stability of AR coatings, which is mainly owing to the lowered porosity and surface energy in the modified coating.

The 532-nm laser damage tests of the silica substrates coated with pure silica and FTG/PMBA-PMMA/silica were performed according to the standard of ISO 11254. The pulse duration is of 10 ns, with a diameter of 916 μm on the sample. Figure 8 shows that damage threshold measured for substrate coated with FTG/PMBA-PMMA/silica AR coating is about 50 J/cm^2. This value can be compared with threshold measurements performed on substrates coated with and without pure silica AR coating which exhibits damage threshold also at the level of about 50 J/cm^2. It is evident that introducing of FTG and PMBA-PMMA compounds does not affect the laser damage threshold of 532 nm obviously.

With the 532-nm laser irradiation and 10-ns pulse duration, some large size defects in the coating or substrate will absorb the energy, and thus the surrounding material may be initiated to change into vapor and plasma. The materials covered on the defects will be ejected out by intensive vapor pressure and plasma shock wave, and hence form damage pits and a number of cracks around the pits[10]. As shown in Fig. 9, the substrate without coating, substrate with pure silica AR coating, and substrate with FTG/PMBA-PMMA/silica AR coating all present damage morphology of material evaporation, damaged pits, and cracks.

In conclusion, as a new coating, FTG/PMBA-PMMA/silica hybrid AR coatings are prepared by a base-catalyzed sol-gel process. By adding FTG into the silica sol, the polarity of the particle surfaces, the porosity and stacking manner of silica particles are controlled. With the increase of FTG/TEOS ratio, the hydrophobicity of the AR coating increases to a certain degree. Modification with PMBA-PMMA increases the hydrophobicity of the coatings due to the lowered polarity and surface energy of the coating as a whole. The modified silica AR coatings retain high transmission of up to 99.6% at a determined wavelength, and possess an improved repellent ability to liquid water and volatile organics in a coarse vacuum. After modification, the laser damage threshold is not obviously affected, and the silica coating with 6% of FTG and 4% of PMBA-PMMA are about 50 J/cm^2 at 532-nm wavelength laser and 10-ns pulse duration.

References

1. I. M. Thomas, Appl. Opt. **25,** 1481 (1986).
2. H. G. Floch and F. P. Belleville, J. Sol-Gel Sci. Technol. **1,** 293 (1994).
3. F. Liu, S. Zhou, W. Dong, and X. Fang, Chin. Opt. Lett. **11,** S10211 (2013).
4. R. Liu, R. Zhan, Y. Tang, and J. Zhu, Chin. Opt. Lett. **4,** 119 (2006).
5. X. Li, and J. Shen, Thin Solid Films **519,** 6236 (2011).
6. X. Zhang, B. Xia, H. Ye, Y. Zhang, B. Xiao, L. Yan, H. Lv, and B. Jiang, J. Mater. Chem. 22, 13132 (2012).
7. R. Shriner, C. Hermann, T. Morrill, D. Curtin, and R. Fuson, *The systematic identification of organic compounds* (in Chinese) S. Zhang, Y. Wen, and C. Ding (trans.) (Chemical Industry Press, Beijing, 2007) 155-161.
8. R. Chen, X. Zhang, Z. Su, R. Gong, X. Ge, H. Zhang, and C. Wang, J. Phys. Chem. C **113,** 8350 (2009).
9. D. Facio and M. Mosquera, Appl. Mater. Interfaces **5,** 7517 (2013).
10. R. Qiu, J. Wang, H. Ren, X. Li, P. Shi, H. Liu, and P. Ma, High Power Laser Particle Beams **24,** 1057 (2012).